Journal of Materials Science: Materials in Electronics (2018) 29:16111–16119
https://doi.org/10.1007/s10854-018-9700-1

Required theoretical and experimental physical characteristics of tris[4-(diethylamino)phenyl] amine organic material

Emine Tanış[1] · Emine Babur Sas[2] · Bayram Gündüz[3] · Mustafa Kurt[4]

Received: 26 March 2018 / Accepted: 18 July 2018 / Published online: 27 July 2018

Abstract
In here, we investigated the required theoretical and experimental physical characteristics such as potential energy surface scan, optimized structure, vibrational spectra, electronic band structure, molecular electrostatic potential surface, optical and optoelectronic behaviors of the tris[4-(diethylamino)phenyl] amine (TDAPA) for different solvents (DMF and chloroform) and techniques (experimental and theoretical). We obtained the significant, interesting, same and different results for them. We obtained the refractive indices of the TDAPA for various conditions. The TDAPA exhibits a normal dispersion behavior in visible region. TDAPA organic material is suitable for optoelectronic devices and applications such as metal–organic semiconductor diodes due to the appropriate properties.

1 Introduction

Over the past decades, researchers and commercialized have focused on the organic light emitting diodes (OLEDs). These materials have a wide application in electrical, electronic, optical, optoelectronic and photonic technology due to its crystal structure, optoelectronic properties, panel displays and lighting applications, easy conductivity control, good environmental stability, corresponding to the visible spectrum, its energy gap of 2.5 eV and low cost manufacturing in large quantities [1–7]. Also these materials have high contrast, low weight, flexibility and they can be rollable or foldable to meet several special needs [8]. These wide possible properties can be realized by analyzing the basic science in involved in the operation the physics of OLEDs. Triphenylamine (TPA) and related derivatives are widely used as three-dimensional conjugated systems of organic semiconductors (OSCs) with superior performance transporting/hole-injecting behavior or luminophore materials in LEDs due to the non-coplanarity geometry of the three phenyl rings [9–11]. TPA-based compounds have been widely applied as electroluminescence and hole transport materials [10, 12–15] and their multifunctional and amorphous properties offer the possibilities to develop active materials for organic fotovoltaic diodes and solar cells with charge transport and isotropic optical properties [12]. On the other hand, tris[4-(diethylamino)phenyl] amine (TDAPA) molecule is used as a dopant of nanostructure film that it increasing carrier concentration [16].

In the present work, we investigated optoelectronic properties of TDAPA molecule for different solvents and molarities. Also, the characterization of the TDAPA molecule was theoretically performed by using the density function theory (DFT) method, as well as in the use of the FT-IR, dispersive Raman, UV–Vis measurements. Experimental and theoretical results were compared to better analysis. Investigation of the spectroscopic and optoelectronic properties of the TDAPA molecule is theoretically and experimentally important for the formation of new OLED materials.

Electronic supplementary material The online version of this article (https://doi.org/10.1007/s10854-018-9700-1) contains supplementary material, which is available to authorized users.

✉ Emine Babur Sas
baburemine@gmail.com

[1] Kaman Vocational Schools, Ahi Evran University, Kırşehir, Turkey

[2] Department of Electronics and Automation, Ahi Evran University, Kırşehir, Turkey

[3] Department of Science Education, Faculty of Education, Muş Alparslan University, 49250 Muş, Turkey

[4] Department of Physics, Ahi Evran University, Kırşehir, Turkey

2 Experimental details

TDAPA organic semiconductor molecule and the solvents of dimethy formamide (DMF), chloroform ($CHCl_3$) solvents were obtained from Sigma-Aldrich. The FT-IR spectra of the headline molecule were taken in the range 500–4000 cm^{-1} with a KBr quartz using a Nicolet 6700 Thermo Scientific and dispersive Raman spectra were recorded for same solvent in the range 100–3500 cm^{-1} with Thermo Scientific. Its UV–Vis absorption spectrum was dissolved in DMF and $CHCl_3$ solvents and recorded in the 200–600 nm range by using Thermo Scientific.

3 Computational details

The molecular structure of TDAPA molecule in the ground state was optimized by DFT method with 6-311G(d,p) basis set using the Gaussian 09 software [17]. The geometric parameters (bond lengths and bond angles), harmonic vibrational frequencies, HOMO–LUMO energy differences, UV–Vis analysis and MEP for this molecule are calculated by using these methods. The obtained frequencies were scaled by 0.967 [18].

4 Results and discussion

4.1 Potential energy surface (PES) scan, optimized structure and vibrational spectra

The potential energy surface (PES) is calculated around the single bonds so that the molecule's optimal structure can be found. Firstly, to find the lowest energy state of in the title molecule, torsional angles were calculated between phenyl ring and N atoms. Rotation around N1–C22 bond (C12–N1–C22–C24). On this calculation, torsion angle was varied from 0° to 360° by changing every 10°, 36 steps were taken. A second torsion angle was calculated after the lowest energy state of the molecule was found. Rotation around C29–N34 bond (C25–C29–N34–C52). On this calculation, torsion angle was also varied from 0° to 360° by changing every 10°, 36 steps were taken. PES for TDAPA molecule were given Fig. 1. The molecular structure of TDAPA molecule in the ground state was optimized and geometric parameters calculated by DFT/B3LYP method with 6-311G(d,p) basis set using the Gaussian 09 software after finding the lowest energy state [17]. The calculated geometric parameter is shown in Table S1 and the theoretical geometric structure in the title molecule is given Fig. S1. TDAPA molecule has 76 atoms and 222 vibrational modes.

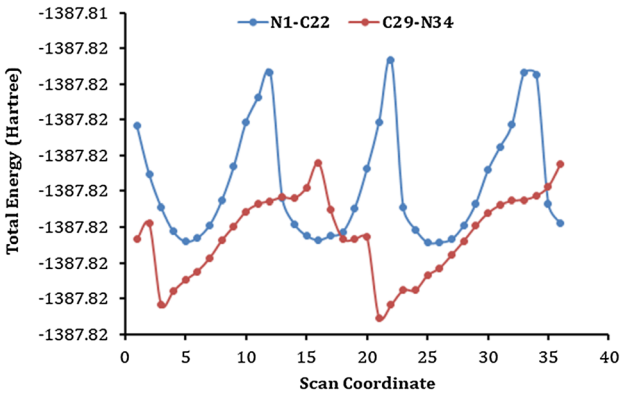

Fig. 1 PES scan for dihedral angle of TDAPA

Spectroscopic properties of the TDAPA molecule were calculated by using same method and all the 222 vibrational modes were found to be IR and Raman active. In order to benchmark between these spectra and theoretical spectra, the using data in Table 1 is visually presented in Fig. 2.

4.2 Optical behaviors of the TDAPA molecule

Absorbance and absorption coefficient are the most significant parameters for optical and optoelectronic technologies and their technological applications. Absorbance (Abs) is dimensionless and its alternative names are molar absorbancy and optical density (OD). Abs can be given by Beer–Lambert law,

$$Abs = ln\left\{\frac{I(0)}{I(L)}\right\} = \varepsilon cL \tag{1}$$

where I(0) is the initial radiant intensity, I(L) is the final radiant intensity, ε is the molar absorptivity, c is the molar concentration and L is the length of the optical path. There are various names for ε constant including absorptivity, molar absorptivity, extinction coefficient, molar extinction coefficient, attenuation coefficient and absorbancy index. But, mostly the molar extinction coefficient and absorptivity expressions are preferred [19–21]. The experimental absorbance and theoretical absorptivity spectra of the TDAPA molecule for DMF and chloroform solvents are shown in Fig. 3a, b, respectively. Theoretical calculations of the TDAPA molecule are made of this TD-DFT/CAM-B3LYP/6-311G(d,p) basis set in DMF, chloroform solvents and gas phase. The calculated and experimental absorption wavelengths, excitation energies and electronic values of the title molecule are given in Table 2. As seen in Fig. 3a, the absorbance and absorptivity spectra of the TDAPA molecule for DMF solvent exhibit maximum peaks at 321 and 296 nm, respectively. Also, these spectra are dominate in near ultraviolet

Table 1 Comparison of the calculated and experimental vibrational spectra and proposal assignments of Tris(4-(diethylamino)phenyl)amine molecule

No	Experimental wavenumbers		Theoretical wavenumber				PED (= 10%)
	FT-IR	Dis-Raman	Scaled[b]	I_{IR}	S_{Ra}	I_{Ra}	Assignments[a]
43		417	415	3.91	2.97	0.040784	Γ_{tors}CCCN (55)
55	559		550	15.28	0.69	0.00514	ϒNCCC (33)
62	704		716	12.52	2.02	0.008195	γ_{str}NC(13)
63	724		718	2.42	1.26	0.005074	γ_{str}NC(13)
66		748	746	17.15	6.06	0.022403	γ_{str}NC(13)
71	808		808	2.45	0.49	0.001502	Γ_{tors}HCNC (11), Γ_{tors}HCCN (19)
80	909	893	910	15.46	17.43	0.040232	γ_{str}CC(20)
94	1005		1021	0.06	1.54	0.002685	Γ_{tors}HCCC (41), Γ_{tors}HCCN (23), Γ_{tors}CCCN (11)
100	1072		1081	5.78	14.01	0.021224	γ_{str}NC(26), γ_{str}CC(30)
105	1093		1100	4.18	2.70	0.003933	γ_{str}CC(10), Γ_{tors}HCNC (22)
111	1153		1152	0.93	0.70	0.000908	γ_{str}CC(20), δ_{bend}HCC(33)
114		1168	1167	157.34	37.00	0.046239	Γ_{tors}HCNC(28)
121	1255		1232	0.37	9.06	0.009847	γ_{str}CC(39), Γ_{tors}HCNC(11)
122		1278	1287	7.92	0.74	0.000723	γ_{str}CC(20), δ_{bend}HCC(33)
123	1282		1289	482.62	36.67	0.035448	γ_{str}CC(10)
129	1326		1324	4.18	79.49	0.071699	δ_{bend}HCC(16)
136	1373		1380	48.88	35.11	0.028396	δ_{bend}HCC(49)
137	1398		1380	8.59	18.49	0.014944	δ_{bend}HCC(43)
138		1391	1381	46.82	22.29	0.018005	δ_{bend}HCC(45)
163	1502		1505	20.79	14.47	0.009261	δ_{bend}HCH(67)
177		1609	1600	5.89	3.45	0.00187	γ_{str}CC(36)
178	1612		1653	17.80	842.12	0.415623	γ_{str}CC(41)
181	2866		2920	98.85	170.34	0.013595	γ_{str}CC(56)
182	2926		2921	75.59	156.83	0.012495	γ_{str}CH(99)
183	2966		2922	120.53	242.95	0.019342	γ_{str}CH(98)
192	3040		3033	40.81	319.08	0.022053	γ_{str}CH(77)

[a] ν stretching, γ out of plane bending, δ in plane-bending, τ torsion, *sm* symmetric, *asm* asymmetric

[b] the vibrational frequencies were computed with the B3LYP/6-311G(d,p) basis set and scaling factor for 6-311G(d,p) was taken as 0.967

(NUV) region. The absorbance and absorptivity values continue almost after a certain wavelength (at about 510 nm). As seen in Fig. 3b, the Abs and ε spectra of the TDAPA molecule for chloroform exhibit maximum peaks at 282 and 295.6 nm, respectively. Similar to DMF solvent, the Abs and ε spectra for chloroform solvent are also dominant in NUV region. As seen in Fig. 3a, b, there are significant, interesting, same and different results for different solvents (DMF and chloroform) and techniques (experimental and theoretical). These results indicate that the absorbance and absorptivity spectra in DMF solvent obtained from experimental and theoretical results are more consistent and stable than that of the related spectra in chloroform. The experimental absorbance and theoretical absorptivity spectra of the TDAPA molecule for DMF and chloroform solvents exhibit two peaks, which one of them corresponds to NUV, other corresponds to V region.

Transmittance (T) is another important parameter for optical and optoelectronic properties, which are crucial for technological applications. The T is given by

$$T = \frac{I(L)}{I(0)} = 10^{-\varepsilon cL} \tag{2}$$

The transmittance spectra of the TDAPA molecule for DMF and chloroform solvents were determined and were indicated in Fig. S2. The T values of the TDAPA molecule are the highest in V region as seen in Fig. S2. We calculated the average (T_{avg}) of the transmittance of the TDAPA molecule for DMF and chloroform solvents and found to be 57.7 and 36.3%, respectively. The T_{avg} values for DMF are higher than that for chloroform due to lower molarity of the solution of the TDAPA molecule in DMF. According to these results, the transmittance spectra of the TDAPA molecule can be controlled with solvents.

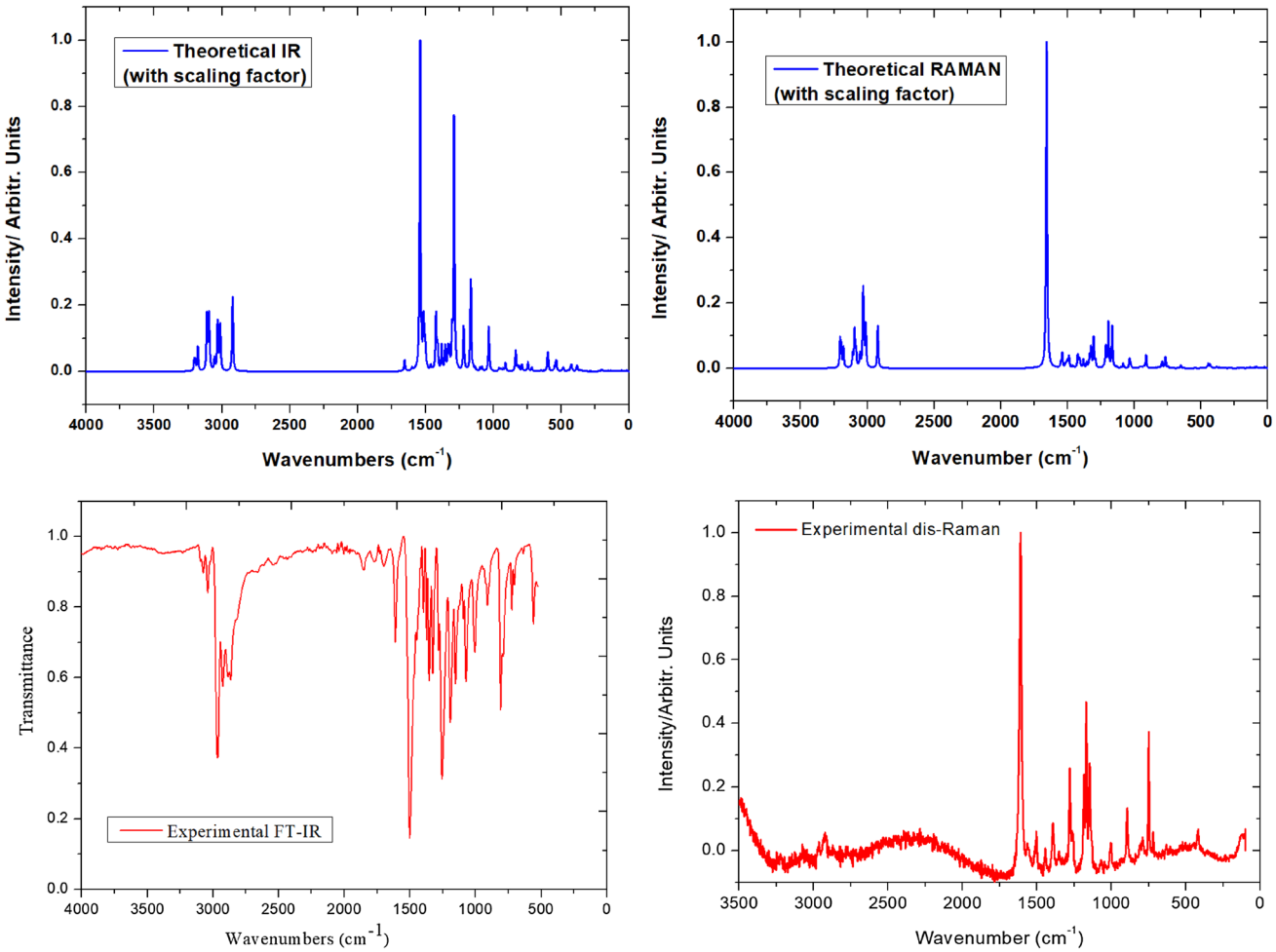

Fig. 2 The experimental and calculated (with the scale factor) FT-IR and dis-Raman spectra of the TDAPA

Optical absorption spectra allow to assign of direct and indirect transition originated from the band of materials [22]. Optical band gap (E_g) is one of the most important optical parameter and can be obtained from Tauc model given [19–21, 23]:

$$\alpha(h\vartheta) = A(h\vartheta - E_g)^{\gamma} \tag{3}$$

where α is absorption coefficient, A is a constant and $h\vartheta$ is the photon energy. The optimal γ value for the TDAPA molecule is the 1/2, which is for allowed direct transition. We estimates the allowed direct E_g values of the TDAPA molecule for DMF and chloroform solvents from the intercept of the linear regions of the $(\alpha h\vartheta)^2$ versus $h\vartheta$ (or E) as seen in Fig. 4. The E_g values of the TDAPA molecule for DMF and chloroform solvents were found to be 2.672 and 2.564 eV, respectively. The E_g value for chloroform is lower than the E_g value for DMF due to higher molarity of the solution of the TDAPA molecule in chloroform. This result is consistent with the related studies [19, 24] in the literature. The availability of allowed direct band gap for the TDAPA molecule is very important to fabricate more efficient optoelectronic devices.

Refractive index (n) based on wavelength is a key feature for performance, controlling and design of the optical and optoelectronic devices and can be completely determined from optical perspective of material [25]. The n can be obtained for various wavelengths based on the light reflectivity theory [26] and is given by,

$$n = \left\{ \sqrt{\frac{4R}{(R-1)^2} - k^2} - \frac{R+1}{R-1} \right\} \tag{4}$$

where R is the reflectance and $k = \alpha\lambda/4\pi$. We calculated the n values of the TDAPA molecule for DMF and chloroform solvents. Figure S3 shows the n curves of the TDAPA molecule for related solvents. The TDAPA molecule exhibits a normal dispersion behavior in V region, in which the n values decrease with increasing wavelength.

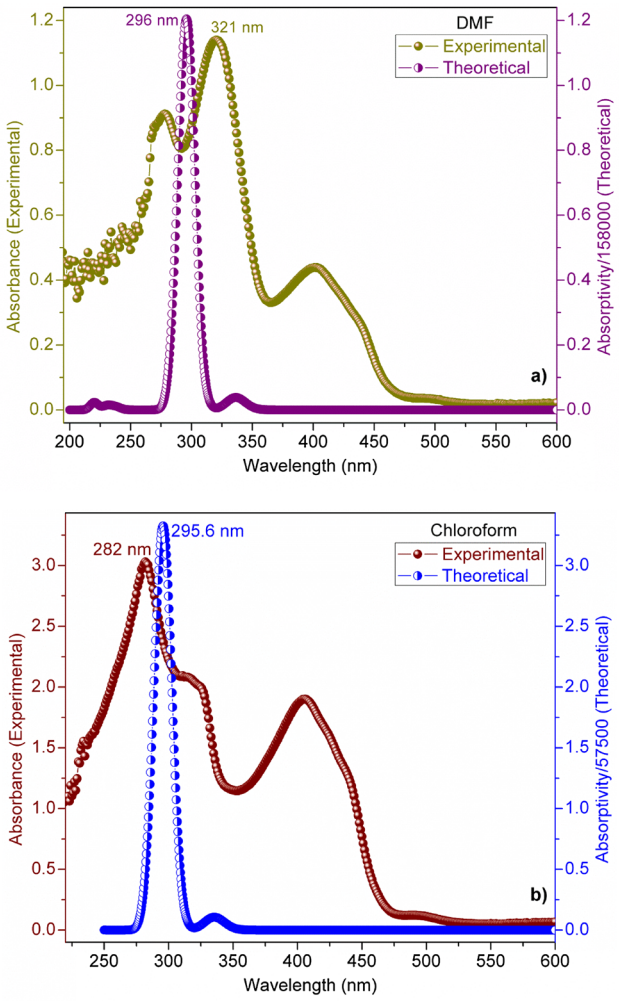

Fig. 3 The experimental absorbance and theoretical absorptivity spectra of the TDAPA molecule for **a** DMF and **b** chloroform solvents

There are many relations such as experimental, Moss et al. [24, 27] to obtain the refractive index based on optical band gaps. We calculated the n values of the TDAPA molecule for DMF and chloroform solvents and for these relations. The n curves versus solvents of the TDAPA molecule for the related relations are indicated in Fig. S4. As seen in Fig. S4, the experimental n value (2.936) is the highest for chloroform solvent, while the experimental n value (2.238) is the lowest for DMF solvent in all relations. Also, we obtained average refractive index (n_{avg}) values for DMF and chloroform solvents. The n_{avg} value (2.624) of the TDAPA molecule for chloroform is higher than the n_{avg} value (2.475) of the TDAPA molecule for DMF solvent.

Angle of incidence (Φ_1) is necessary to investigate its effects on the operation [28] and external quantum efficiency (EQE) [29] of the optical and optoelectronic devices such as solar cells [30, 31]. The Φ_1 expression can

Table 2 The experimental and computed [TD-DFT/CAM-B3LYP/6-311(d,p)] absorption wavelength λ (nm), excitation energies E(eV), absorbance and oscillator strengths (f) of TDAPA molecule

Theoretical								Experimental			
Chloroform			Gas			DMF		DMF		Chloroform	
λ (nm)	E (eV)	f	λ (nm)	E (eV)	f	λ (nm)	E (eV)	f	λ (nm)	E (eV)	λ (nm)	E (eV)
399.69 (125 → 126)	3.1020	0.0227	394.61 (125 → 126)	3.1420	0.0165	401.47 (125 → 126)	3.0883	0.0224	401	3.0919	–	–
339.54 (125 → 127) (125 → 128)	3.6515	0.5810	334.85 (125 → 128) (125 → 129)	3.7026	0.1258	340.18 (125 → 127) (125 → 128)	3.6447	0.5333	321	3.8624	–	–
338.31 (125 → 128)	3.6560	0.1916	333.71 (125 → 127) (125 → 130)	3.7154	0.2677	339.14 (125 → 128)	3.6558	0.1918	–	–	282	4.3966

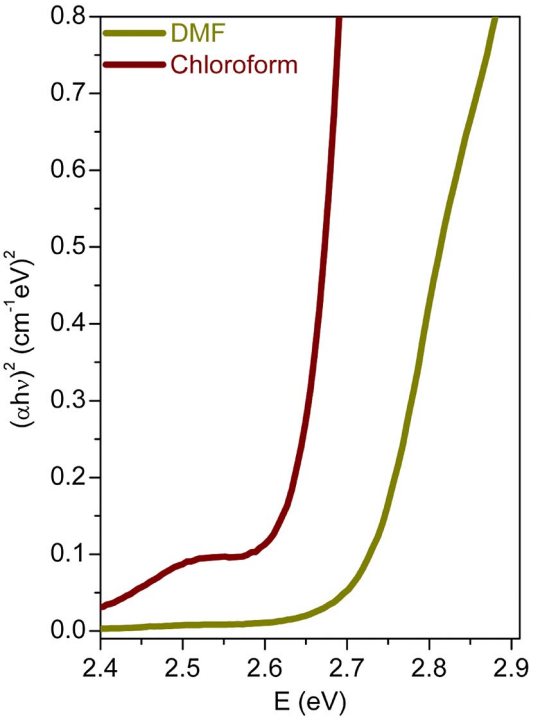

Fig. 4 The $(\alpha h\vartheta)^2$ curves versus $h\vartheta$ of the TDAPA molecule for DMF and chloroform solvents

be calculated by the refractive index of the medium, which is n_1, and n_2 of the material by [19, 32]:

$$\Phi_1 = \tan^{-1}\left(\frac{n_2}{n_1}\right) \tag{5}$$

The Φ_1 values of the TDAPA molecule for DMF and chloroform solvents were obtained. Figure 5a shows the Φ_1 curves versus photon energy (E). The angle values of incidence vary from about 55°–89.5°.

The determination of the angle of refraction (Φ_2) plays role on optical and optoelectronic applications. The Φ_2 can be obtained by [19, 33]:

$$\Phi_2 = \sin^{-1}\left(\frac{n_1}{n_2}\sin\Phi_1\right) \tag{6}$$

We obtained the Φ_2 values of the TDAPA molecule for DMF and chloroform solvents. Figure 5a indicates the Φ_2 curves versus E. The angle values of refraction vary from about 0.5°–35°. As seen in Fig. S5a, the Φ_1 values are higher that the Φ_2 values. This result is an expected situation and consistent with the related studies [19, 34] in the literature.

The reflectance features as a function of the angle of incidence offer important opportunities in optoelectronic efficiency. For this, we plotted the R curves versus Φ_1 of the TDAPA molecule for DMF and chloroform solvents, as seen in Fig. S5b. Reflectance values of the TDAPA molecule

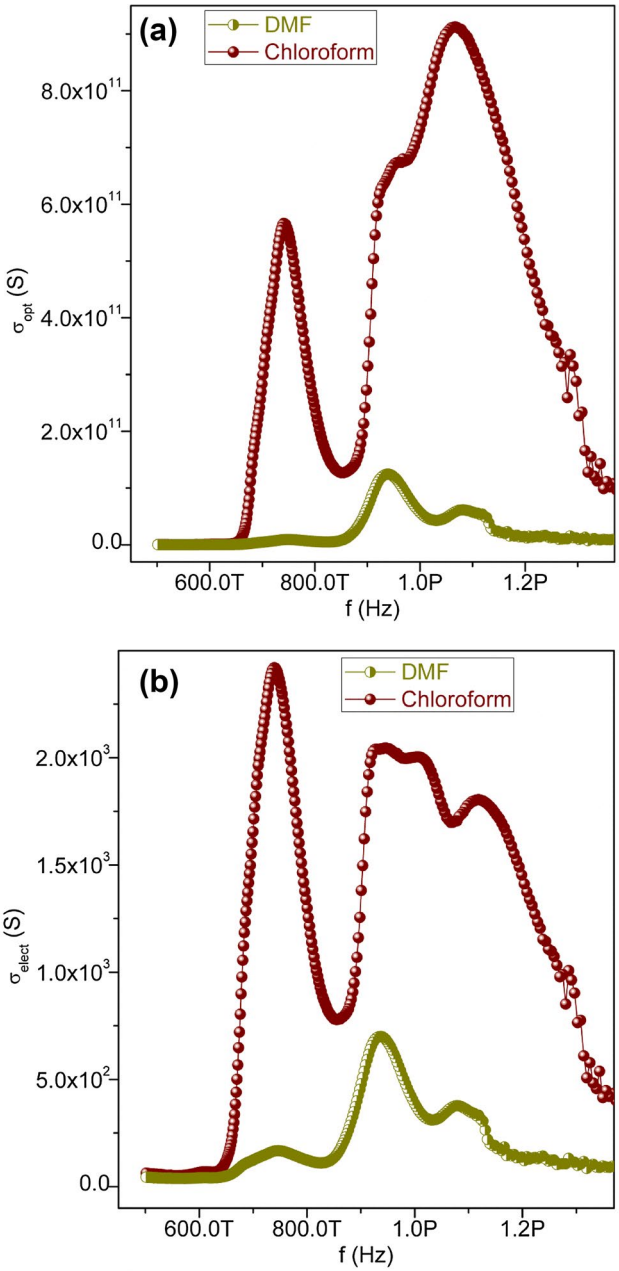

Fig. 5 The **a** σ_{opt} and **b** σ_{elect} curves versus frequency of the TDAPA molecule for DMF and chloroform solvents

increase with increasing angle of incidence are almost the same for both solvents.

The optical conductance (σ_{opt}) and electrical conductance (σ_{elect}) play critical role on physical properties for high performance electronic and optoelectronic applications. The σ_{opt} and σ_{elect} expressions can be obtained from the following equations [20, 24]:

$$\sigma_{opt} = \frac{\alpha nc}{4\pi} \tag{7}$$

where c is the velocity of light and

$$\sigma_{elect} = \frac{2\lambda\sigma_{opt}}{\alpha} \quad (8)$$

We calculated the σ_{opt} and σ_{elect} values of the TDAPA molecule for DMF and chloroform solvents. Figure 5a, b shows the σ_{opt} and σ_{elect} plots versus frequency (f). As seen in Fig. 5a, b, the optical conductance of the TDAPA molecule is maximum in order of about *PHz*, while the electrical conductance of the TDAPA molecule is maximum in order of about *THz*. Also, the optical conductance values are higher than the electrical conductance values. Obtained results show that the σ_{opt} and σ_{elect} values for chloroform are higher than the σ_{opt} and σ_{elect} values for DMF solvent due to lower molarity of the solution of the TDAPA molecule in DMF.

4.3 Electronic band structure

HOMO and LUMO energy levels are important in electrical and optical terms [35]. This energy levels for TDAPA molecule in gas phase and DMF, chloroform solvents computed by using TD-DFT/B3LYP/6-311G(d,p). The energy gap of HOMO and LUMO is found to be 3.76, 3.71 and 3.72 eV in gas phase and DMF, chloroform solvents respectively. As shown in Table 3, the LUMO energy level in the solvent is seen as the lowest DMF. From the results, one can conclude that DMF solvent with the lowering of the band gaps can be preferred for optoelectronic applications or devices, which prefer lower band gaps because the electronic transfer in the molecule TDAPA is easier. Figure 6 shows the energy values of HOMO and LUMO orbital in gas phase. The HOMO orbitals is localized in the whole of molecule and LUMO orbitals is localized in the whole of molecule except CH_3 molecules. Having a molecular low-lying LUMO energy level means that it has high electron attention. This indicates that the molecule has the potential to electron-transporting (n-type) materials for OLED applications [36]. In addition, the chemical hardness, chemical potential, electrophilicity index and electronegativity values belonging to the molecule are seen in Table 2.

4.4 Molecular electrostatic potential surface

2D contour map provides predicting the interaction of different geometries [37–40]. 2D contour map and 3D molecular electrostatic potential surface for TDAPA were drawn and given in Fig. S6. The negative (red) regions and positive (blue) regions show electrophilic reactivity and nucleophilic reactivity, respectively.

The color code maps for the title compound were predicted in between of − 0.03351 (deepest red) and 0.03351 a.u. (deepest blue). Figure 6 indicates that the region around the nitrogen atoms linked with carbon through the single bond is the most electrophilic reactivity (red) and the hydrogen atom linked with carbon atoms is the most of nucleophilic reactivity (blue).

5 Conclusion

In the present study, we have examined PES molecular structure and vibrational wave numbers of TDAPA using DFT/B3LYP/6-311G(d,p) level. FT-IR and dis-Raman spectra and UV–Vis spectrum of molecule were compared with the experimental values, showing a very good agreement. MEPs contour/surface and HOMO–LUMO graphics were drawn to the understanding of attributes and dynamics of the molecule. We compared the UV spectra of the TDAPA for various conditions. The average refractive index value (2.624) of the TDAPA molecule for chloroform is higher than the average refractive index

Table 3 The calculated energies values of TDAPA using by the TD-DFT/B3LYP method using 6-311G(d,p) basis set

C_1 symmetry	Gas	DMF	Chloroform
E_{total} (Hartree)	− 1387.82265171	− 1387.83317405	− 1387.82970188
E_{HOMO} (eV)	− 4.06	− 4.36	− 4.25
E_{LUMO} (eV)	− 0.30	− 0.65	− 0.53
E_{HOMO-1} (eV)	− 5.20	− 5.42	− 5.34
E_{LUMO+1} (eV)	− 0.19	− 0.14	− 0.03
$E_{HOMO-1-LUMO+1\ gap}$ (eV)	**5.01**	**5.27**	**5.31**
$E_{HOMO-LUMO\ gap}$ (eV)	**3.76**	**3.71**	**3.72**
Chemical hardness (h)	1.88	1.85	1.86
Electronegativity (χ)	− 2.18	− 2.50	− 2.39
Chemical potential (μ)	2.18	2.50	2.39
Electrophilicity index (ω)	1.26	1.69	1.53

Bold indicates the most important electronic energy level transition

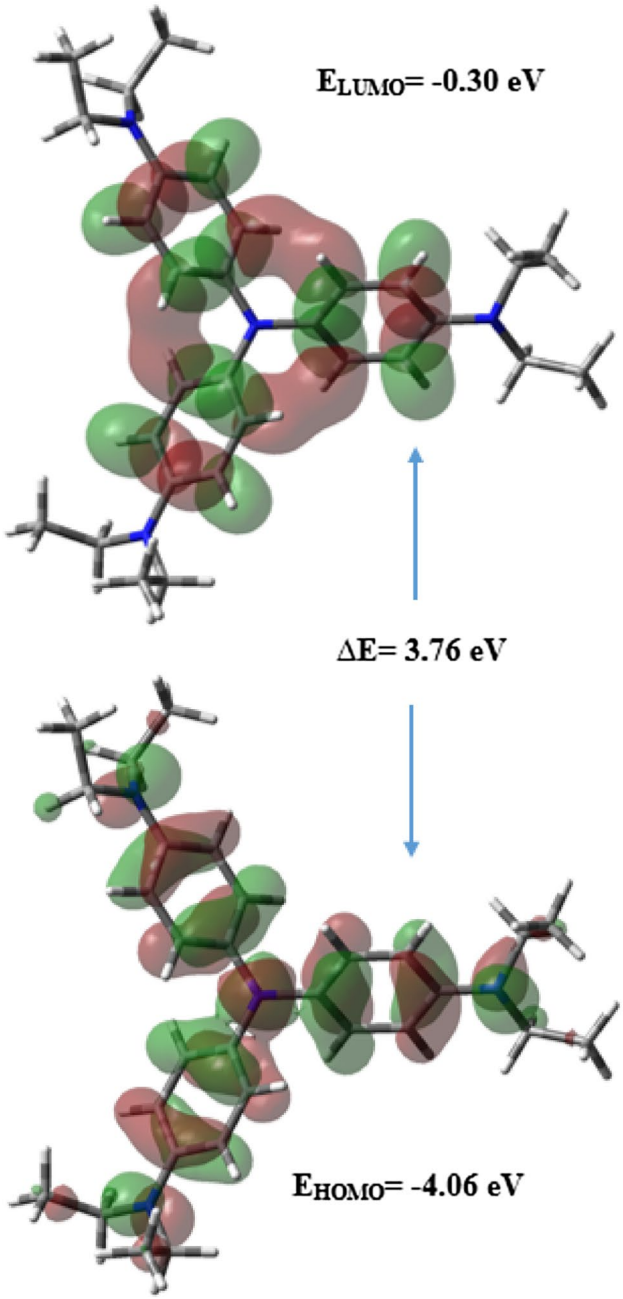

Fig. 6 The frontier molecular orbitals of the TDAPA for gas phase. (Color figure online)

value (2.475) of the TDAPA molecule for DMF solvents. Obtained results suggest that the TDAPA molecule can be used in preparations of the photonic devices and diodes.

Acknowledgements This work was supported by Ahi Evran University Scientific Project Unit (BAP) with, Project No: PYO–FEN.4001.15.012.

References

1. S. Reineke, F. Linder, G. Schwartz, N. Seidler, K. Walazer, B. Lüssem, K. Leo, White organic light-emitting diodes with fluorescent tube efficiency. Nature **459**, 234 (2009)
2. F. So, J. Kido, P. Burrows, Organic light-emitting devices for solid-state lighting. MRS Bull **33**, 663 (2008)
3. T. Nakayama, K. Hiyama, K. Furukawa, H. Ohtani, Development of phosphorescent white OLED with extremely high power efficiency and long lifetime. J. SID **16**(2), 231–236 (2008). https://doi.org/10.1889/1.2841855
4. J. Chen, F. Zhao, D. Ma, Hybrid white OLEDs with fluorophors and phosphors. Mater. Today **17**, 175 (2014)
5. J. Lee, W.J. Sung, C.W. Joo, H. Cho, N.S. Cho, G.-W. Lee, D.-H. Hwang, J.-I. Lee, Simplified bilayer white phosphorescent organic light-emitting diodes. ETRIJ **38**, 260 (2016)
6. F. Wudl, G. Srdanov, US Patent 51,891,36A, 1993
7. A. Ltaief, A. Bouazizi, J. Davenas, R.B. Chaabane, H.B. Ouada, Electrical and optical properties of thin films based on MEH-PPV/fullerene blends. Synth. Met. **147**, 261 (2004)
8. B. Geffroy, P. Roy, C. Prat, Review organic light-emitting diode (OLED) technology:materials, devices and display technologies. Polym. Int. **55**, 572–582 (2006)
9. A. Cravino, P. Leriche, O. Alévêque, S. Roquet, J. Roncali, Light-emitting organic solar cells based on a 3d conjugated system with internal charge transfer. Adv. Mater. **18**, 3033–3037 (2006)
10. Y. Shirota, Photo- and electroactive amorphous molecular materials molecular design, syntheses, reactions, properties, and applications. J. Mater. Chem. **15**, 75–93 (2005)
11. M.M. Stylianakis, J.A. Mikroyannidis, Q.F. Dong, J.N. Pei, Z.Y. Liu, W.J. Tian, Synthesis, photophysical and photovoltaic properties of star-shaped molecules with triphenylamine as core and phenylethenylthiophene or dithienylethylene as arms. Sol. Energy Mater. Sol. Cells **93**, 1952–1958 (2009)
12. M. Zhang, Z. Wu, Q. Wang, Q. Song, Y. Ding, Synthesis and properties of a new [60] fullerene-donor system containing dicyanovinyl groups. Mater. Lett. **64**, 2244–2246 (2010)
13. Y.J. Shirota, Organic materials for electronic and optoelectronic devices. Mater. Chem. **10**(1), 1–25 (2000)
14. K. Walzer, B. Maennig, M. Pfeiffer, K. Leo, Highly efficient organic devices based on electrically doped transport layers. Chem. Rev. **107**, 1233–1271 (2007)
15. H.P. Zeng, T.T. Wang, S.D. Sandanayaka, Y. Araki, O.J. Ito, Photoinduced charge separation and charge recombination in [60]fullerene-ethylcarbazole and [60]fullerene-triphenylamines in polar solvents. J. Phys. Chem. A **109**, 4713–4720 (2005)
16. P. Drzaic, D. Hecht, M. O'Connell, G. Irvin, US Patent 2009/0169819 A1, 2009
17. M.J. Frisch, G.W. Trucks, H.B. Schlegel, G.E. Scuseria, M.A. Robb, J.R. Cheeseman, G. Scalmani, V. Barone, B. Mennucci, G.A. Petersson, H. Nakatsuji, M. Caricato, X. Li, H.P. Hratchian, A.F. Izmaylov, J. Bloino, G. Zheng, J.L. Sonnenberg, M. Hada, M. Ehara, K. Toyota, R. Fukuda, J. Hasegawa, M. Ishida, T. Nakajima, Y. Honda, O. Kitao, H. Nakai, T. Vreven, J.A. Montgomery Jr., J.E. Peralta, F. Ogliaro, M. Bearpark, J.J. Heyd, E. Brothers, K.N. Kudin, V.N. Staroverov, R. Kobayashi, J. Normand, K. Raghavachari, A. Rendell, J.C. Burant, S.S. Iyengar, J. Tomasi, M. Cossi, N. Rega, J.M. Millam, M. Klene, J.E. Knox, J.B. Cross, V. Bakken, C. Adamo, J. Jaramillo, R. Gomperts, R.E. Stratmann, O. Yazyev, A.J. Austin, R. Cammi, C. Pomelli, J.W. Ochterski, R.L. Martin, K. Morokuma, V.G. Zakrzewski, G.A. Voth, P. Salvador, J.J. Dannenberg, S. Dapprich, A.D. Daniels, O. Farkas, J.B. Foresman, J.V. Ortiz, J. Cioslowski, D.J. Fox (2009) Gaussian 09, revision A.02. Gaussian Inc, Wallingford, CT

18. E.B. Sas, M. Kurt, M. Can, N. Horzum, A. Atac, Spectroscopic studies on 9H-Carbazole-9-(4-phenyl) boronic acid pinacol ester by DFT method. J. Mol. Struct. **1118**, 124–138 (2016)
19. B. Gündüz, Effects of molarity and solvents on the optical properties of the solutions of tris[4-(5-dicyanomethylidenemethyl-2-thienyl)phenyl]amine (TDCV-TPA) and structural properties of its film. Opt. Mater. **36**(2), 425–436 (2013)
20. C. Orek, B. Gündüz, O. Kaygili, N. Bulut, Electronic, optical, and spectroscopic analysis of TBADN organic semiconductor: experiment and theory. Chem. Phys. Lett. **678**, 130–138 (2017)
21. M. Kurban, B. Gündüz, Physical and optical properties of DCJTB dye for OLED display applications: experimental and theoretical investigation. J. Mol. Struct. **1137**, 403–411 (2017)
22. S.B. Aziz, O. Gh.Abdullah, M.A. Rasheed, A novel polymer composite with a small optical band gap: new approaches for photonics and optoelectronics. J. Appl. Polym. Sci. **134**, 44847 (2017)
23. M.M. El-Nahass, A.M. Farid, A.A. Atta, Structural and optical properties of Tris(8-hydroxyquinoline) aluminum (III)(Alq3) thermal evaporated thin films. J. Alloy Compd. **507**, 112–119 (2010)
24. M. Cabuk, B. Gündüz, Controlling the optical properties of polyaniline doped by boric acid particles by changing their doping agent and initiator concentration. Appl. Surf. Sci. **424**, 345–351 (2017)
25. R.H. French, J.M. R-Parada, M.K. Yang, R.A. Derryberry, N.T. Pfeiffenberger, Optical properties of polymeric materials for concentrator photovoltaic systems. Sol. Energy Mater. Sol. Cells **95**, 2077–2086 (2011)
26. S.B. Aziz, M.A. Rasheed, A.M. Hussein, H.M. Ahmed, Fabrication of polymer blend composites based on $[PVA\text{-}PVP]_{(1-x)}:(Ag_2S)_x$ $(0.01 \leq x \leq 0.03)$ with small optical band gaps: structural and optical properties. Mater. Sci. Semicond. Process. **71**, 197–203 (2017)
27. S.K. Tripathy, Refractive indices of semiconductors from energy gaps. Opt. Mater. **46**, 240–246 (2015)
28. M.S.S. Rahman, M.K. Alam, Effect of angle of incidence on the performance of bulk heterojunction organic solar cells: a unified optoelectronic analytical framework. AIP Adv. (2017). https://doi.org/10.1063/1.4985049.
29. G. Dennler, K. Forberich, M.C. Scharber, C.J. Brabec, I. Tomiˇs, K. Hingerl, T. Fromherz, Angle dependence of external and internal quantum efficiencies in bulk-heterojunction organic solar cells. J. Appl. Phys. **102**, 054516 (2007)
30. A. Meyer, H. Ade, The effect of angle of incidence on the optical field distribution within thin film organic solar cells. J. Appl. Phys. **106**, 113101 (2009)
31. S. Lee, I. Jeong, H.P. Kim, S.Y. Hwang, T.J. Kim, Y.D. Kim, J. Jang, J. Kim, Effect of incidence angle and polarization on the optimized layer structure of organic solar cells. Sol. Energy Mater. Sol. Cells **118**, 9 (2013)
32. F. Abelès (ed.), *Optical Properties of Solids* (North-Holland, Amsterdam, 1972)
33. S. Adachi, *Optical Constants of Crystalline and Amorphous Semiconductors: Numerical Data and Graphical Information*, (Kluwer Academic Publishers, London, 1999)
34. B. Gündüz, Optical properties of poly[2-methoxy-5-(3′,7′-dimethyloctyloxy)-1,4-phenylenevinylene] light-emitting polymer solutions: effects of molarities and solvents. Polym. Bull. **72**(12), 3241–3267 (2015)
35. E.B. Sas, M. Cevik, M. Kurt, Experimental and theoretical analysis of 2-amino 1-methyl benzimidazole molecule based on DFT. J. Mol. Struct. **1149**, 882–892 (2017)
36. H. Ulla, M.R. Kiran, B. Garudachari, T.N. Ahipa, K. Tarafder, A.V. Adhikari, G. Umesh, M.N. Satyanarayan, Blue emitting 1,8-naphthalimides with electron transport properties for organic light emitting diode applications. J. Mol. Struct. **1143**, 344–354 (2017)
37. E. Scrocco, J. Tomasi, Electronic molecular structure, reactivity and intermolecular forces: an euristic interpretation by means of electrostatic molecular potentials. Adv. Quantum Chem. **11**, 115–121 (1978)
38. C. Muñoz-Caro, A. Niño, M.L. Sement, J.M. Leal, S. Ibeas, Modeling of protonation processes in acetohydroxamic acid. J. Org. Chem. **65**, 405–410 (2000)
39. P. Politzer, K.C. Daiker, Chap. 6. Models for chemical reactivitiy, ed. by D.M. Deb. *The Force Concept In Chemistry*, (Van Nostrand Reinhold Co., New York, 1981)
40. P. Politzer, P.R. Laurence, K. Jayasuriya, J. McKinney, Structure activity correlation in mechanism studies and predictive toxicology. Spec. Issue Environ. Health Perspect. **61**, 191 (1985)